Am J Transl Res 2017;9(7):3200-3211
www.ajtr.org /ISSN:1943-8141/AJTR0055433

*Original Article*

# Restoration of bone defects using modified heterogeneous deproteinized bone seeded with bone marrow mesenchymal stem cells

Jun Li, Zeyu Huang, Liyan Chen, Xin Tang, Yue Fang, Lei Liu

*Department of Orthopaedics, West China Hospital, Sichuan University, 37# Wainan Guoxue Road, Chengdu 610041, People's Republic of China*

Received January 25, 2017; Accepted June 20, 2017; Epub July 15, 2017; Published July 30, 2017

**Abstract:** The aim of the present study was to investigate the effect of modified heterogeneous deproteinized bone combined with bone marrow mesenchymal stem cells (BMSCs) in the restoration of a validated bone defect model. BMSCs were identified by flow cytometry and multilineage differentiation assay. The structural features of the modified heterogeneous deproteinized bone scaffold and biocompatibility between BMSCs and the scaffold were confirmed by scanning electron microscope (SEM) detection. The cytotoxicity of the modified heterogeneous deproteinized bone scaffolds were detected by 3-(4,5-dimethylthiazol-2-yl)-2,5-diphenytetrazolium bromide (MTT) assay. SEM detection proved that modified heterogeneous deproteinized bone scaffold had no negative impact on the proliferation of BMSCs. MTT assay results demonstrated that the scaffold had no apparent cytotoxicity. Biomechanical detection showed that the stiffness and ultimate loading of tibias in the scaffold + BMSCs group were significantly higher than those of the scaffold alone group ($P < 0.05$) and the control group ($P < 0.01$). Histological analyses confirmed that the greatest quantity of new bone was generated in the scaffold + BMSCs group, when compared with all other groups, at 8 weeks' post-operation. The bone mineral density (BMD) in the scaffold + BMSC group was significantly higher than that of the scaffold alone group ($P < 0.05$) and the control group ($P < 0.01$). Fluorometric analyses confirmed the presence of BMSCs at high concentration within the bone defect areas in the scaffold + BMSCs group at 4 weeks after transplantation. These findings suggest that the modified heterogeneous deproteinized bone scaffold seeded with BMSCs can effectively enhance the restoration of bone defects.

**Keywords:** Bone defect, modified, heterogeneous deproteinized bone, BMSCs

## Introduction

Bone defects caused by traumatic events, correction of congenital malformation, or resection of tumors are commonly encountered issues in a clinical setting [1, 2]. Given these conditions, the development of a reasonable intervention to accelerate bony reconstruction and achieve osseous union is of great importance [3]. Despite extensive research, the restoration of long-bone defects deriving from these pathological processes remains challenging [4, 5].

The most frequently adopted material in current bone transplantation clinical practice is autologous bone [6]. Autologous bone prevails not only because it is safe, inexpensive, and easy to obtain, but it also possesses osteoconduction and osteoinduction characteristics [7]. Nevertheless, the application of autologous grafts requires patients to suffer additional operations, which are associated with extra morbidity at the harvesting site and increased operational costs. Furthermore, the graft material is limited in quantity and may increase the risk of complications at the donor site, such as stress fractures, infections, and cacesthesia [8]. Hence, it is imperative to overcome these limitations and explore novel biomaterials for bone grafts. Fortunately, heterogeneous deproteinized bone, which possesses similar organizational structures to the human skeleton, can serve as a good alternative [9]. Besides, the osteoconductive and osteoinductive characteristics of this material potentially fulfill the de-

mand of an optimal bony transplantation substitute [10]. Previous research conducted by Urist et al. [11] confirmed the feasibility of heterogeneous deproteinized bone matrices as scaffolds for tissue-engineering applications. The bone-derived growth factors in the heterogeneous deproteinized bone, together with the architectural and mechanical properties and unlikelihood of triggering immunological reactions, make it a suitable osteoinductive biomaterial [11].

Mesenchymal stem/stromal cells (MSCs) that can be isolated from bone marrow, umbilical cord, and other organs can be extensively expanded in vitro [13]. MSCs are further characterized by their self-renewal and multi-directional differentiation potential; under certain conditions, they can differentiate into osteocytes, chondrocytes, tendon cells, adipocytes, and other cell types [14-16]. Bone formation in the course of embryogenesis is initiated by MSC accumulation and recruitment, which then develops to intramembranous bone formation by means of osteogenic differentiation, or to endochondral bone formation through chondrogenic differentiation [17]. Although MSCs are rare in adult bone, interrelated osteoprogenitor cells derived from the periosteum, together with primitive multiply differentiative MSCs derived from bone marrow, engage in callus formation, which is significant during the architectural progress of fracture concrescence [17]. Moreover, the homing capacity of bone marrow mesenchymal stem cells (BMSCs) to the injured area, with their paracrine effect facilitating cell migration and accelerating angiogenesis, and their immunoregulation characteristics, making them an ideal therapeutic option in the reconstruction of long bone defects [19]. Several studies have demonstrated significant restoration effects of orthotopically implanted or pre-seeded BMSCs on various biomaterials in critical size bone defect models [6, 20-23]. Studies by Haynesworth et al. [6, 20-23] showed that ceramic scaffolds seeded with human BMSCs could expedite bone tissue formation in immunodeficient mice, which supplied proof-of-principle on the practicability of employing BMSCs in bone tissue engineering.

Based on the above information, we proposed a distinct concept using modified heterogeneous deproteinized bone seeded with bone marrow mesenchymal stem cells in the repair of bone defects in a validated rat model.

## Materials and methods

### *Animals*

Forty healthy adult female Sprague-Dawley (SD) rats, weighing 250-300 g and aged approximately 12 weeks, were used for the present study. The animals were housed in an indoor facility for 1 week before the start of the experiments, with accessible food and water in conditions of 21°C, 60% atmospheric humidity, and a 12 h light/dark cycle. All animal experimental procedures were approved by the Ethics Committee for Animal Experiments of the West China School of Medicine, Shichuan University, Chengdu, China (SCXK20150012).

### *Isolation, cultivation, and labeling of BMSCs*

Primary BMSCs were separated from the bone marrow of young adult male Sprague-Dawley rats in accordance with previously described protocols [25]. In brief, rats were anaesthetized with 10% chloral hydrate (0.3 mL/100 g), after which the tibias and femurs were dissected. The metaphyses of each bone were removed, and medullary cavities were douched with 10 mL BMSC culture medium, containing α-minimal essential medium (α-MEM; HyClone, Utah, USA), 10% fetal bovine serum (FBS; Biological Industries, Kibbutz Beit Haemek, Israel), and penicillin (Amresco, OH, USA). The cells were filtered via a 70-μm cell strainer, centrifuged at 1000 rpm for 5 minutes, and then cultivated at a concentration of 5-10 × $10^5$ cells/$cm^2$ in BMSC nutrient medium. Cells were incubated at 37°C in a humidified environment with 5% $CO_2$ for 24 hours, and non-adherent cells were eliminated. The medium was replaced every 2 days until the adherent cells reached 80-90% confluence. Subsequently, the BMSCs were detached with trypsin and serially subcultured three times at 1:3. To track the internal activity of BMSCs, they were also dyed with a cell tracker (CM-DiI, Invitrogen, California, USA) according to the manufacturer's instructions. The BMSC suspension was irrigated using phosphate buffered saline (PBS) and cocultured with CM-DiI (2 μg/mL) at 37°C for 5 minutes, then incubated at 4°C for 15 minutes. The BMSCs were then washed twice using PBS and resuspended in α-MEM for use in further experiments.

*Flow cytometry assay*

BMSCs were suspended in PBS (Beyotime Institute of Biotechnology, Shanghai, China) containing 5% bovine serum albumin (BSA; HyClone, Utah, USA) at a density of $1 \times 10^6$ cells/mL. Cell suspensions (500 μL) were transferred to 4 Eppendorf tubes (1.5 mL), one of which was used as a control, then centrifuged at 1000 rpm for 5 minutes before the supernatant was discarded. Paraformaldehyde solution (4%, 0.1 mL) was added to each tube and fixed for 30 minutes. The cells were washed with BSA/PBS buffer as above, centrifuged at 1000 rpm for 5 minutes, and the supernatant was discarded. This process was repeated 3 times. The cells were dyed with fluorescein isothiocyanate (FITC)-conjugated antibodies specific for CD29 and CD45 (both eBioscience, CA, USA) at 4°C for 30 minutes. The cells were also incubated with phycoerythrin (PE)-conjugated antibodies against CD44 (R&D Systems, Minnesota, USA) at 4°C for 30 minutes. The cells were washed with BSA/PBS buffer, centrifuged at 1000 rpm for 5 minutes and the supernatant was discarded. This process was repeated 3 times. The immunophenotype of the cells was analyzed by fluorescence-activated cell sorting flow cytometry (BD Biosciences, New Jersey, USA).

*Multilineage differentiation assay*

BMSCs at passage 3 were adjusted to a density of $1 \times 10^5$ cells/mL in Dulbecco's modified Eagle's medium (DMEM; Invitrogen, California, USA) containing 10% FBS, and inoculated into 24-well culture plates. For adipogenic induction, Oil red O staining was performed. The inductive medium consisted of 10 mg/L insulin, 0.5 mM 3-isobutyl-1-methylxanthine (IBMX; New Jersey, USA), 50 μM indomethacin, 0.1 μmol/L dexamethasone, α-MEM, and 10% FBS. The medium was changed every 72 hours, and the cells were stained with Oil red O solution at day 14. For osteoinductive differentiation, alkaline phosphatase (ALP) staining was carried out. The inductive medium consisted of α-MEM, 10% FBS, 10 mmol/L sodium β-glycerophosphate, 0.25 μmol/L dexamethasone, and 50 μmol/L ascorbic acid. The osteoinductive medium was changed every 72 hours, and cells dyed positive for ALP were observed using a light microscope at day 21.

*Preparation of heterogeneous deproteinized bone scaffold*

The heterogeneous deproteinized bone scaffold was fabricated in accordance with previously recorded protocols, with certain modifications [26, 27]. The hypomeres and spongy bone of adult swine tibias were obtained from a fresh produce market in Neijiang City (Wuhou District, Chengdu, China), and the peripheral soft tissue, bone marrow, and cartilage were then removed. The bones were cut into block-shapes consistent with the bone trabecular direction, with dimensions of 3 mm × 3 mm × 5 mm, which were comprised of porous and cortical bone tissues. After washing with physiological saline several times, the blocks were immersed in 0.3 mg/mL pepsin (NCE Biomedical Co., Ltd., Wuhan, China) dissolved in pH 2 PBS (Beyotime Institute of Biotechnology, Shanghai, China) at 25°C for 8 hours. The reaction was subsequently terminated by altering the pH to 9 using NaOH solution. Sequentially, the materials were soaked in 5 mmol/L $NaN_3$ for 12 hours, 0.25% trypsin at 4°C for 6 hours, 0.6 N hydrochloric acid at room temperature for 4 hours, methanol/chloroform (1:1) at room temperature for 12 hours, and then in 0.5% sodium dodecyl sulfate (SDS; Leica Biosystems, Shanghai, China) at room temperature for 6 hours. Each procedure was followed by sufficient irrigation using distilled water. The deproteinized bones were frozen in a cryogenic refrigerator at -85°C for 3 months and then sterilized by $^{60}Co$ irradiation. The resultant scaffolds were stored at -4°C until evaluation by scanning electronic microscopy and for BMSC implantation.

*Pre-seeding of BMSCs into heterogeneous deproteinized bone scaffold*

The previously prepared scaffolds were disinfected with 75% ethyl alcohol for 24 hours, then irrigated three times with PBS and soaked in BMSC culture medium (DMEM) for another day before seeding. The redundant medium was removed from the scaffolds and BMSC suspensions ($5 \times 10^6$/mL) were slowly and carefully seeded into the porous scaffolds. The composites were incubated with 5% $CO_2$ at 37°C for 3 hours. BMSCs were further incubated with the scaffolds in culture medium at 100% humidity and 37°C for 7 days; the medium was renewed every 48 hours.

*MTT assay*

The cytotoxicity of heterogeneous deproteinized bone scaffolds was detected by MTT assay (Beyotime Institute of Biotechnology, Beijing, China). First, the heterogeneous deproteinized bone scaffolds were disinfected with 75% ethyl alcohol for 24 hours, then irrigated with PBS three times. After soaking in 10 mL DMEM complete medium at 5% $CO_2$ and 37°C for 72 hours, the extract liquid was then adjusted to 50% and 100% relative concentration. BMSCs at passage 3 in DMEM were seeded at a density of $1 \times 10^4$ cells/mL into 96-well plates in 50% and 100% extract liquid, and without extract liquid (medium only) as controls. MTT (10 μL) was added on days 1, 3, 5, and 7 during the cultivation, the samples were incubated at 37°C for 4 hours, and then the medium was substituted with 100 μL dimethyl sulfoxide (DMSO; Sigma-Aldrich, Darmstadt, Germany). The formazan crystals were dissolved through low speed oscillation for 10 minutes, and the optical density (OD) of each well was subsequently measured at 490 nm in an absorbance reader (Beckman Coulter, Inc., California, USA). The average OD values and relative proliferation ratio (RPR) of each group was calculated relative to the control group.

*SEM detection*

After gold sputtering, the characteristics of the heterogeneous deproteinized bone scaffolds were detected using SEM (Amray Inc., MA, USA), and the pore size and porosity of samples were calculated using Labworks™ image analysis system. After coculturing with BMSCs for 7 days (as previously described), the scaffolds were washed with PBS and fixed in 2.5% glutaric dialdehyde for 3 hours. The composites were washed with PBS, dried and coated, then observed with SEM.

*Operative procedure for tibia defect model*

SD rats were anesthetized by administering 10% chloral hydrate (0.3 mL/100 g) intraperitoneally, and the left hind limbs were shaved and sterilized with alcohol. Incisions were made posteromedial of the tibia, and the subcutaneous tissues and muscular layers were blunt-dissected to expose the tibia. Five millimeter long bone defects were created using a bone saw, and the corresponding graft material was implanted according to the grouping. The rats were randomly divided into three groups (n = 12 per group). The defects were left unfilled in the control group, the heterogeneous deproteinized bone scaffolds were pressed into the defects for the scaffold group, and the heterogeneous deproteinized bone scaffolds with preseeded BMSCs were pressed into the defects for the scaffold + BMSCs group. Muscle and skin were sutured layer by layer, and all operating procedures were conducted under aseptic conditions. The tibias were harvested separately at 4 weeks and 8 weeks and fixed in 10% formaldehyde solution for further analysis.

*Biomechanical detection*

For biomechanical detection, six rats from each group were assessed at 8 weeks after operation. The specimens were harvested and the soft tissues were removed, after which the biomechanical properties of stiffness (N/mm) and ultimate loading (N) were determined using a universal biomechanics tester (RGT-5A, Ruige Technology Co., Ltd, Shenzhen, China). The data are plotted as mean ± SD.

*Histological and histomorphometric analyses*

Tibia specimens from each group, retrieved after sacrifice at 4 weeks and 8 weeks, were fixed in 10% formalin solution and decalcified with ethylenediaminetetraacetic acid (EDTA; Invitrogen, CA, USA). After dehydration through a graded ethanol series (80%-100%), the specimens were embedded in paraffin. The longitudinal region of the tibia defect was cut into 5 μm thick sections and dyed using hematoxylin and eosin (H&E) or Masson's trichrome. After microscopic inspection, photographs of the stained sections were taken with a digital camera (70D, Canon, Tokyo, Japan), and the obtained images were stored in the computer for histomorphometric analysis. The sizes of newly generated bone regions and the amount of new blood vessels within the bone defect regions were estimated with automatic image analysis software (Image-Pro Plus, Meyer Instruments, Inc., Houston, Texas, USA). The ratio of new bone formation was calculated as the percentage of newly generated bone region over the total defect region. The neovascular density was calculated as the amount of new blood vessels over the total defect region.

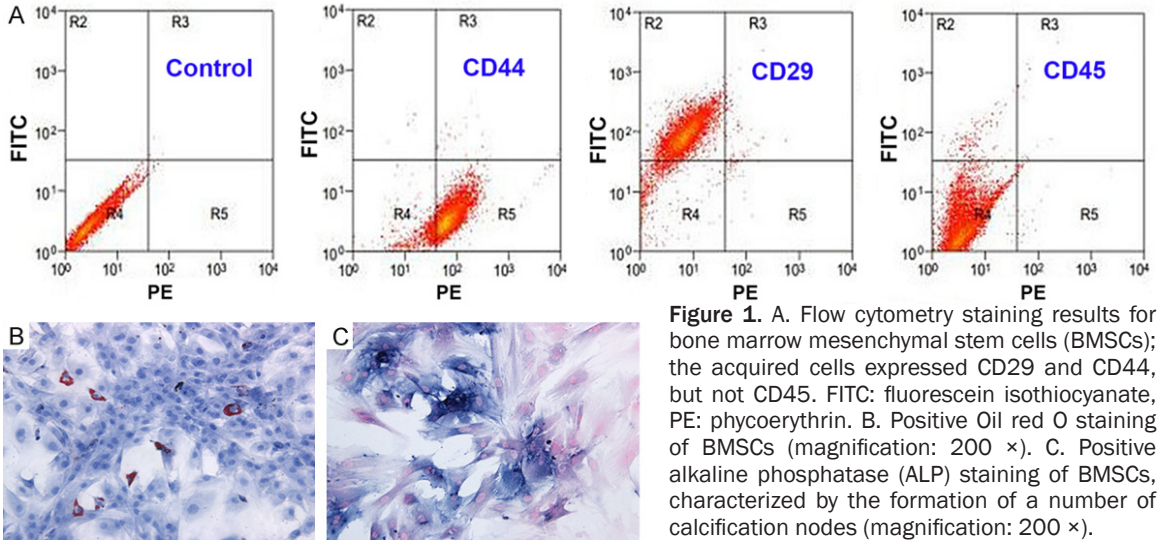


**Figure 1.** A. Flow cytometry staining results for bone marrow mesenchymal stem cells (BMSCs); the acquired cells expressed CD29 and CD44, but not CD45. FITC: fluorescein isothiocyanate, PE: phycoerythrin. B. Positive Oil red O staining of BMSCs (magnification: 200 ×). C. Positive alkaline phosphatase (ALP) staining of BMSCs, characterized by the formation of a number of calcification nodes (magnification: 200 ×).

*Micro-computed tomography detection*

To evaluate the newly formed mineralized tissue, the rat tibias were scanned and analyzed using micro-computed tomography (micro-CT, Quantum GX, Japan) at 8 weeks' post-operation. The percentage of newly formed mineralized bone volume of the defect tissue volume (BV/TV) and bone mineral density (BMD) of the regenerated bone were calculated as previously described [28].

*Fluorescence microscopy*

Four weeks after operation, bone defect specimens were frozen and embedded in OCT compound (Leica Biosystems, Shanghai, China), and then cut into 7 μm longitudinal cryostat sections. Fluorometric analyses were carried out using immunofluorescent microscopy to determine the existence or absence, as well as the relative density, of CM-DiI-labeled BMSCs in the defect areas.

*Statistical analysis*

Statistical analyses were performed using Statistical Package for the Social Sciences (SPSS; 19.0, IBM, NYC, USA). All data were expressed as the mean value ± standard deviation (SD). Multiple group comparison was conducted using analysis of variance (ANOVA), followed by Bonferroni or Dunnett post-hoc tests. If significance was reached, an unpaired two-tailed Student's t-test was performed between each compared population, unless otherwise indicated. $P < 0.05$ was considered statistically significant.

## Results

*Identification and multilineage differentiation of BMSCs*

Immunophenotype analysis by flow cytometry showed that the cells we acquired were strongly positive for CD29 and CD44, while negative for CD45, which is in accordance with the characteristics of BMSCs (**Figure 1A**). Multilineage differentiation capacity of BMSCs was evaluated by subjecting BMSCs to adipogenic and osteogenic differentiation protocols and dying for lipids and mineralization respectively. After incubation of BMSCs in adipogenic inductive medium for 14 days, positive Oil red O staining was observed (**Figure 1B**), indicating the adipogenic differentiation of BMSCs. The cells cultivated in osteogenic inductive medium for 21 days generated a large number of mineral nodules (**Figure 1C**), indicating the osteogenic differentiation of BMSCs into osteoblasts.

*Heterogeneous deproteinized bone scaffold has no negative impact on the proliferation of BMSCs*

Characteristics of the heterogeneous deproteinized bone scaffolds and biocompatibility between BMSCs and the scaffolds were detected by SEM. The results showed that the heterogeneous deproteinized bone retained a three-dimensional porous structure and network porosity that were similar to those of natural bone. Pores connected with each other and the porosity rate was 79.6 ± 5.39% with an aperture size of 446.10 ± 7.35 μm (**Figure 2A**). After cocultivation for 7 days, the BMSCs

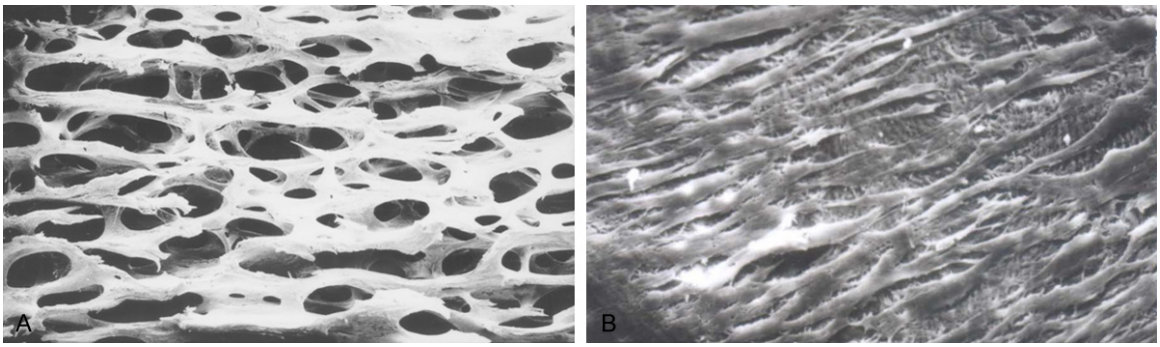


**Figure 2.** Scanning electron microscope (SEM) detection results (magnification: 500 ×). A. three-dimensional porous structure of heterogeneous deproteinized bone showing pores connected with each other. B. After cocultivation for 7 days, bone marrow mesenchymal stem cells (BMSCs) adhered, proliferated, and generated extracellular matrix on the heterogeneous deproteinized bone scaffold surfaces.

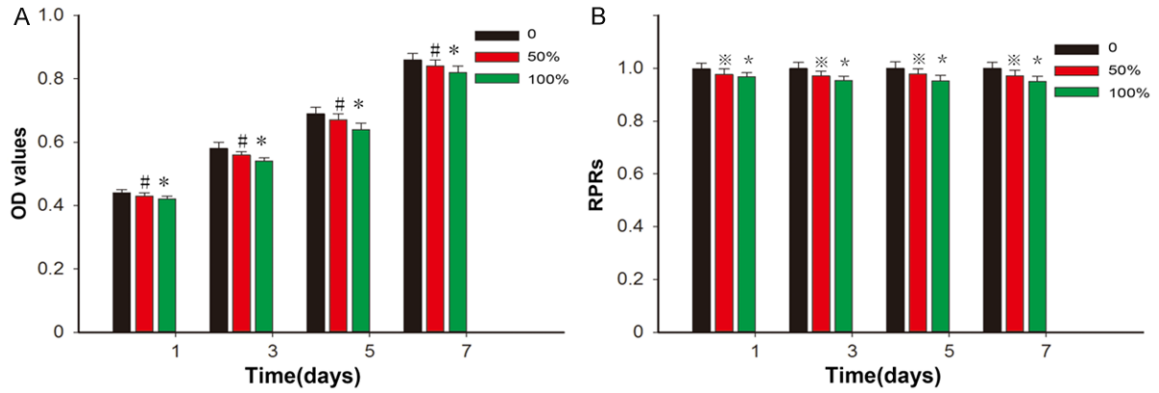


**Figure 3.** Cytotoxicity analyses and relative proliferation ratio (RPR) of bone marrow mesenchymal stem cells (BMSCs) on heterogeneous deproteinized bone scaffolds. A. OD values in 0, 50% and 100% extracted liquid, #P > 0.05 versus control group, *P > 0.05 versus control group. B. RPRs of BMSCs in each group, ※P > 0.05 versus control group, *P > 0.05 versus control group. The data are plotted as mean ± SD.

adhered, proliferated, and generated extracellular matrix on the heterogeneous deproteinized bone scaffold surfaces (**Figure 2B**), which indicated that the chemical constitution and structural features of the scaffolds have no negative impact on the proliferation of BMSCs.

*Heterogeneous deproteinized bone scaffold shows no apparent cytotoxicity to BMSCs*

The proliferation of BMSCs in liquid extracted from heterogeneous deproteinized bone scaffold culture was detected using MTT assay on days 1, 3, 5, and 7. As shown in **Figure 3A**, during the 7 days' cultivation, the OD values in each group increased, indicating increasing cell counts, and this further demonstrated that the heterogeneous deproteinized bone scaffold has no apparent cytotoxicity to BMSCs. The OD values in 50% and 100% extracted liquid groups were less than that of basic medium, but the difference was not significant ($P > 0.05$). There was no significant difference with regard to RPRs of BMSCs between the extracted liquid group and the control group ($P > 0.05$) (**Figure 3B**).

*Tibia defects treated with scaffold and BMSCs has higher stiffness and ultimate loading*

The results of biomechanical detection at 8 weeks after operation are shown in **Figure 4**. The stiffness of tibias in the scaffold alone group (61.02 ± 3.38 N/mm) was significantly higher than that of the control group (43.88 ± 2.94 N/mm), ($P < 0.05$) (**Figure 4A**). The tibia defects treated with heterogeneous deproteinized bone scaffold + BMSCs were mechanically stronger than those of the other groups (79.64 ± 4.25 N/mm), significantly higher than those of the scaffold alone group ($P < 0.05$) and the control group ($P < 0.01$). The ultimate loading of tibias in the scaffold alone group (9.16 ± 0.73 N) was significantly higher than those of the

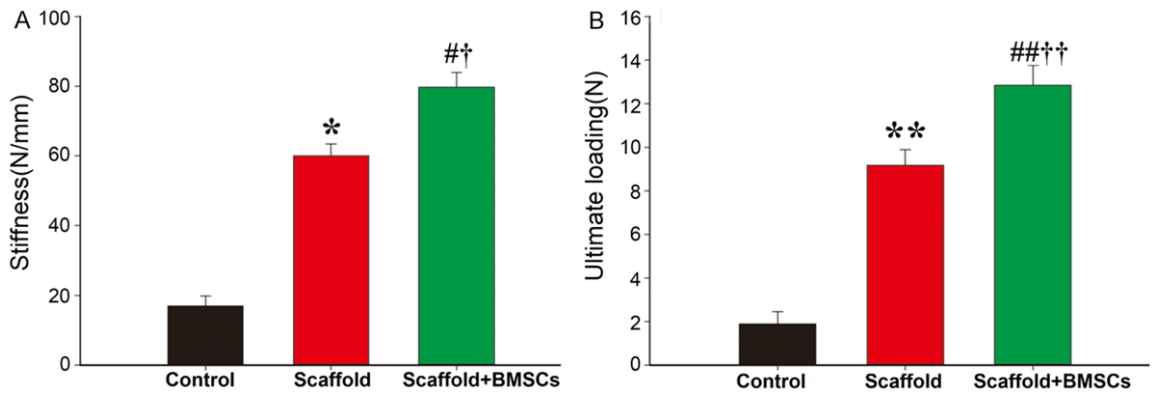


**Figure 4.** Results of biomechanical detection at 8 weeks after operation. A. Tibial stiffness in each group. #P < 0.05 versus control group; †P < 0.05 versus scaffold group; *P < 0.01 versus control group. B. Ultimate loading of tibias in each group. ##P < 0.05 versus scaffold group; ††P < 0.01 versus control group, **P < 0.05 versus control group. The data are plotted as mean ± SD.

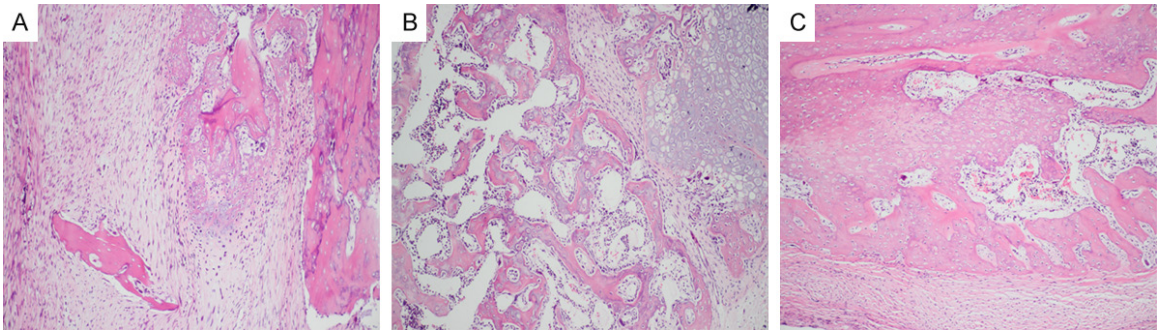


**Figure 5.** Histological examination of newly regenerated bone at 8 weeks after operation. Representative H&E images (magnification: 100 ×). New bone areas were stained in pink/red. A. Control group; B. Scaffold group; C. Scaffold + BMSCs group. Inflammatory reactions were not observed in any group. BMSCs, bone marrow mesenchymal stem cells.

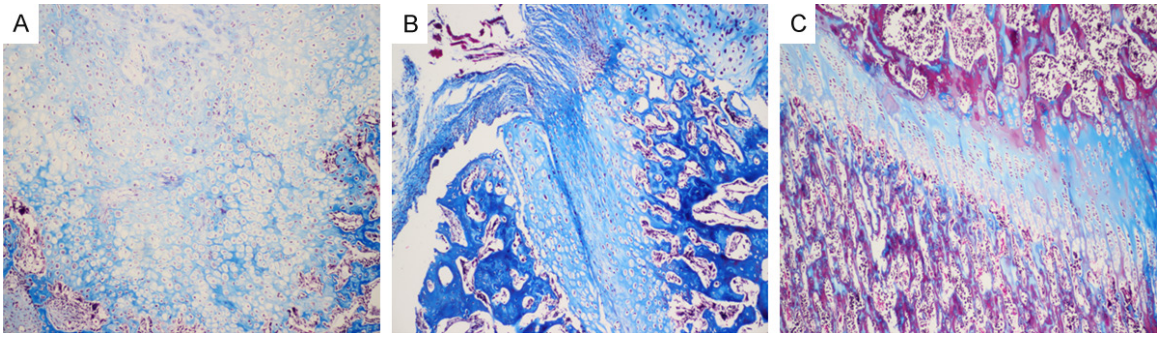


**Figure 6.** Representative Masson's trichrome staining images (magnification: 100 ×). A. Control group; B. Scaffold group; C. Scaffold + BMSCs group. BMSCs, bone marrow mesenchymal stem cells.

control group (7.65 ± 0.67 N), (P < 0.05) (**Figure 4B**). The ultimate loading of tibias in the scaffold + BMSCs group (12.83 ± 0.92 N) was significantly higher than those of the scaffold alone group (P < 0.05) and the control group (P < 0.01).

*The tibia defects treated with scaffold and BMSCs had larger amounts of new bone and greater neovascular density*

Bone regeneration in the defect areas was evaluated at 8 weeks' post-operation, and rep-

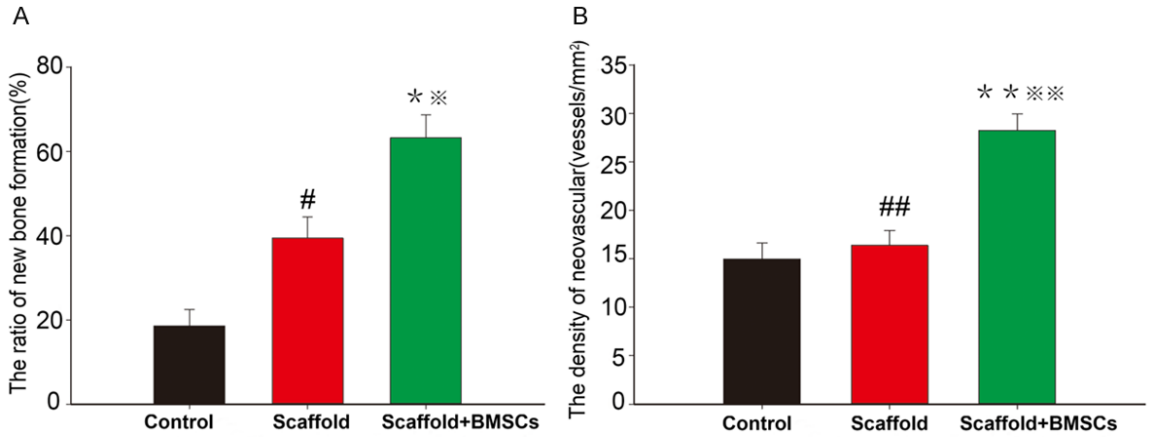


**Figure 7.** The ratio of new bone formation and the neovascular density at 8 weeks after operation in each group. A. Ratio of new bone formation, $^{*}P < 0.05$ versus scaffold alone group, $^{※}P < 0.01$ versus control group, $^{\#}P < 0.05$ versus control group. B. Neovascular density, $^{**}P < 0.01$ versus scaffold alone group, $^{※※}P < 0.01$ versus control group, $^{\#\#}P > 0.05$ versus control group. The data are plotted as mean ± SD.

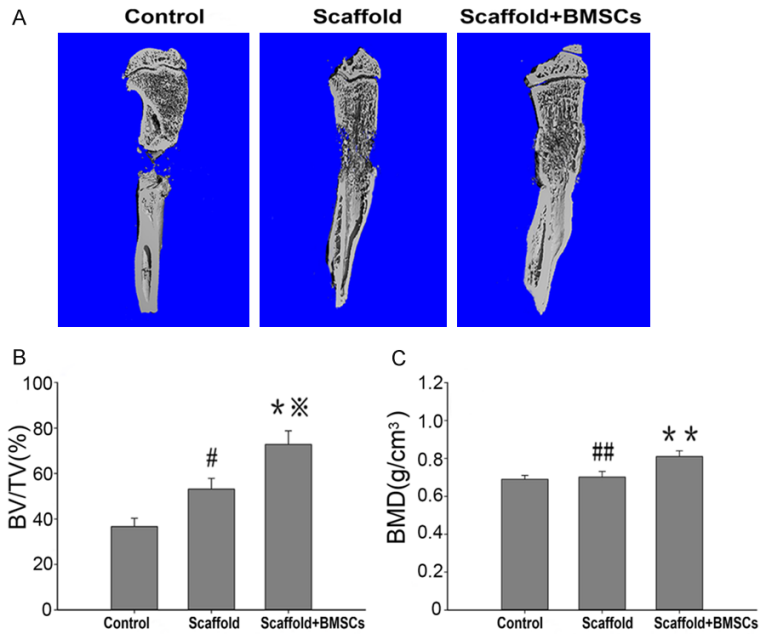


**Figure 8.** Micro-CT 3D reconstruction and quantitative results of tibia defects at 8 weeks. A. Both the scaffold and scaffold + BMSCs groups showed extensive new bone formation. B. BV/TV in the bone defect area, $^{*}P < 0.05$ versus scaffold group, $^{※}P < 0.01$ versus control group, $^{\#}P < 0.05$ versus control group. C. BMD of newly formed mineralized bone, $^{**}P < 0.01$ versus scaffold alone and control groups, $^{\#\#}P > 0.05$ versus control group. The data are plotted as mean ± SD. BMSCs, bone marrow mesenchymal stem cells.

resentative H&E images are shown in **Figure 5**. New bone areas were stained in pink/red. The control group showed minimal new bone formation in the defect area along with fibrous connective tissue (**Figure 5A**). In contrast, a significant amount of new bone and bone proteins appeared among the defect areas in the scaffold group, along with a certain number of new blood vessels (**Figure 5B**). The highest amounts of new bone were generated in the scaffold + BMSCs group, where some of the new bone exhibited an organized and mature skeletal morphology (**Figure 5C**).

Masson's trichrome staining was also performed to identify the presence of bone tissue in the specimens at 8 weeks' post-operation. Representative Masson's staining images of new bone formation in each group are shown in **Figure 6**. Only minimal amounts of new bone formation were observed in the control group (**Figure 6A**). The new bone in the scaffold alone group appeared to be less mature, with a light red staining that demonstrates an earlier stage of mineralization (**Figure 6B**). There was significantly more new bone formation in the scaffold + BMSCs group than the scaffold alone group and the control group (**Figure 6C**). In addition, the new bone in the scaffold + BMSCs group appeared to be more mature, with a darker red staining that indicates a relatively higher degree of mineralization.

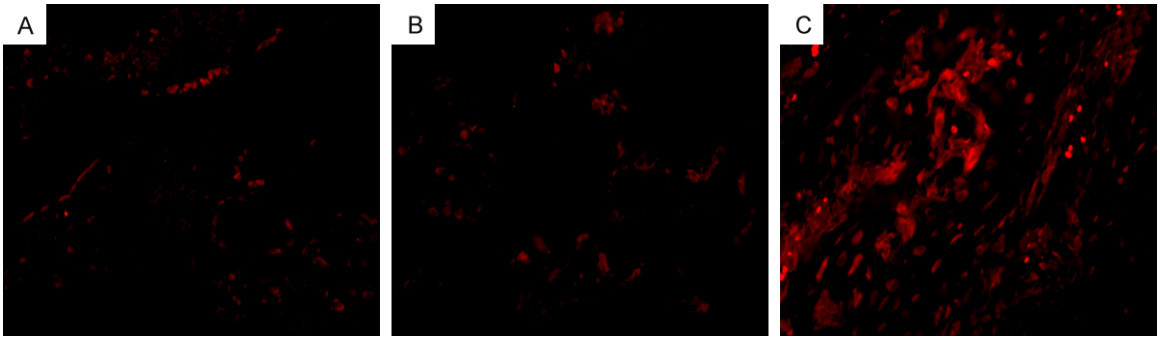


**Figure 9.** Fluorescent imaging within the defect areas of specimens from each group after 4 weeks (magnification: 400 ×). A. Control group; B. Scaffold group; C. Scaffold + BMSCs group. BMSCs, bone marrow mesenchymal stem cells.

The bone generative capability in each group was estimated by calculating the size of the newly generated bone regions with histomorphometry. At 8 weeks after operation, the ratio of new bone formation in the scaffold alone group (39.42 ± 5.03%) was significantly higher than that of the control group (18.51 ± 3.98%), ($P < 0.05$) (**Figure 7A**). The ratio of new bone formation in the scaffold + BMSCs group (53.20 ± 5.47%) was significantly higher than those of the scaffold alone group ($P < 0.05$) and the control group ($P < 0.01$). The neovascular density in the scaffold alone group was higher than that of control group, but the difference was not statistically significant ($P > 0.05$) (**Figure 7B**). The neovascular density in the scaffold + BMSCs group was significantly higher than those of the scaffold alone group ($P < 0.01$) and the control group ($P < 0.01$).

*Tibia defects treated with scaffold and BMSCs have higher BV/TV ratios and BMD*

The newly formed mineralized bone volume in each group was estimated through three-dimensional CT reconstruction at 8 weeks' postoperation (**Figure 8A**). The defects remained discontinuous in the control group. In contrast, the scaffold and scaffold + BMSCs groups showed massive amounts of newly formed bone with bridge connection of the defects After 8 weeks, the BV/TV in the scaffold + BMSC group was significantly higher than those of the scaffold group ($P < 0.05$) and the control group ($P < 0.01$) (**Figure 8B**). The BV/TV in the scaffold alone group was significantly higher than that of the control group ($P < 0.05$). In addition, the BMD in the scaffold + BMSCs group was higher than those of the other groups ($P < 0.05$) (**Figure 8C**), while the difference between the scaffold group and the control group was not statistically significant ($P > 0.05$).

*CM-Dil-labeled BMSCs colonized the bone defect areas*

Fluorescent labeling within the defect areas of specimens in each group was analyzed after 4 weeks. Gross and histologic fluorescent imaging found that few CM-Dil-labeled cells were detected in specimens from the control group (**Figure 9A**) and the scaffold alone group (**Figure 9B**). In contrast, the images demonstrated the presence of CM-Dil-labeled BMSCs in high concentration within the bone defect areas in the scaffold + BMSCs group at 4 weeks after transplantation (**Figure 9C**).

## Discussion

Bone rehabilitation follows an extraordinarily coordinated course that is well-orchestrated by a sequence of biological events, generating new bone through osteoinduction and osteoconduction, rather than cicatrical fibrosis [26, 29, 30]. Osteogenesis during embryo formation is initiated by the aggregation and condensation of MSCs, which subsequently develops into endochondral ossification via chondrogenesis, or to intramembranous ossification via osteogenic differentiation [31]. Mechanical stability may modulate the cytoskeletons, integrins, and molecular pathways corresponding to the cellular differentiation and angiogenesis that are involved in the bone formation process [32]. Despite the well-established natural mechanism of bone regeneration, there are many factors, such as the defect position, size, biomechanical conditions, inflammation, underlying diseases, and physical conditions, that can in-

fluence the therapeutic recovery of bone defects [17, 33, 34]. Therefore, exploring valid strategies to optimize bone defect regeneration and reestablish skeletal function is of vital importance.

For an ideal scaffold material in bone tissue engineering, one of the critical characteristics is interconnected pore structures with ample pore size for cell localization, matrix fluxion, vascular formation, and new tissue growth [35, 36]. Scaffold materials like hydroxyapatite (HA) [37], poly (lactide-co-glycolide) [29], and calcium phosphate ceramic composites were developed to mimic the host extracellular matrix on account of their prominent biocompatibility [38, 39]. Nevertheless, these materials do not possess properties, such as hydration and a 3-D porous network that are comparable to host bone, or the capacity to readily integrate biophysical or biochemical signals to induce the function of grafted cells [40]. Heterogeneous deproteinized bone fabricated from natural bone is superior for its inherited characteristics of the primary source materials, including its porous structure [41]. It has been proved that the immunogenicity of heterogeneous deproteinized bone is thoroughly eliminated, since all organic materials are removed by stepwise physical and chemical processing [42]. Until now, this sort of inorganic material has been widely employed in various medical research and clinical applications, such as vertebrae fusion, alveolar bone crest augmentation, and periodontal osseous defect restoration [42]. The optimal outcome of tissue engineering bone is that both the chemical constituents and porosity should sustain cellular migration, differentiation, proliferation, and vascular formation without evoking immune reaction, and degradation over time should occur without toxic metabolites [45]. Consistently, the results of in vitro experiments demonstrated that BMSCs adhered, proliferated, and generated extracellular matrix on the scaffolds' surfaces, which further confirmed the absence of cytotoxicity of heterogeneous deproteinized bone.

Nevertheless, several limitations do exist in the present study. Firstly, the small number of experimental animals is not enough to avoid selection bias. Secondly, we merely observed one time point (eight weeks after operation), instead of a longer observation period, since the primary intention of this study was to detect the early healing of defected bone. In any case, we aim to address the aforementioned limitations in later research.

## Conclusions

In the present study, we modified the manufacturing process of heterogeneous deproteinized bone scaffolds, maintaining the three-dimensional porous structure and network porosity of natural bone. The scaffolds pre-seeded with BMSCs showed good mechanical properties and biocompatibility. Moreover, the modified heterogeneous deproteinized bone scaffold with BMSCs produced good therapeutic effects in a rat model of tibia defects. These findings may provide new information for the further development of bone tissue engineering.

## Acknowledgements

This study was supported by the science and technology support project of Sichuan province, China (2012FZ0044) and Natural Science Foundation of China (81472061).

## Disclosure of conflict of interest

None.

## Authors' contribution

Jun Li performed the experiments and wrote the manuscript. Lei Liu and Jun Li conceived and designed the study. Zeyu Huang, Liyan Chen, Xin Tang and Yue Fang analyzed the data. All authors reviewed the final manuscript.

**Address correspondence to:** Dr. Lei Liu, Department of Orthopaedics, West China Hospital, Sichuan University, 37# Wainan Guoxue Road, Chengdu 610041, People's Republic of China. E-mail: mrorthopedics@sina.com

## References

[1] Arvidson K, Abdallah BM, Applegate LA, Baldini N, Cenni E, Gomez-Barrena E, Granchi D, Kassem M, Konttinen YT, Mustafa K, Pioletti DP, Sillat T, Finne-Wistrand A. Bone regeneration and stem cells. J Cell Mol Med 2011; 15: 718-746.

[2] Wu G, Pan M, Wang X, Wen J, Cao S, Li Z, Li Y, Qian C, Liu Z, Wu W, Zhu L, Guo J. Osteogenesis of peripheral blood mesenchymal stem cells in self assembling peptide nanofiber for

healing critical size calvarial bony defect. Sci Rep 2015; 5: 1-12.
[3] Dong Y, Zhang Q, Li Y, Jiang J, Chen S. Enhancement of tendon-bone healing for anterior cruciate ligament (ACL) reconstruction using bone marrow-derived mesenchymal stem cells infected with BMP-2. Int J Mol Sci 2012; 13: 13605-13620.
[4] Gomez-Barrena E, Rosset P, Muller I, Giordano R, Bunu C, Layrolle P, Konttinen YT, Luyten FP. Bone regeneration: stem cell therapies and clinical studies in orthopaedics and traumatology. J Cell Mol Med 2011; 15: 1266-1286.
[5] Escacena N, Quesada-Hernandez E, Capilla-Gonzalez V, Soria B, Hmadcha A. Bottlenecks in the efficient use of advanced therapy medicinal products based on mesenchymal stromal cells. Stem Cells Int 2015; 2015: 895714.
[6] Hoffman MD, Xie C, Zhang X, Benoit DS. The effect of mesenchymal stem cells delivered via hydrogel-based tissue engineered periosteum on bone allograft healing. Biomaterials 2013; 34: 8887-8898.
[7] Pang KM, Um IW, Kim YK, Woo JM, Kim SM, Lee JH. Autogenous demineralized dentin matrix from extracted tooth for the augmentation of alveolar bone defect: a prospective randomized clinical trial in comparison with anorganic bovine bone. Clin Oral Implants Res 2016; 1: 1-7.
[8] Ng MH, Duski S, Tan KK, Yusof MR, Low KC, Rose IM, Mohamed Z, Bin SA, Idrus RB. Repair of segmental load-bearing bone defect by autologous mesenchymal stem cells and plasma-derived fibrin impregnated ceramic block results in early recovery of limb function. Biomed Res Int 2014; 2014: 1-11.
[9] Šponer P, Strnadová M, Urban K. In vivo behaviour of low-temperature calcium-deficient hydroxyapatite: comparison with deproteinised bovine bone. Int Orthop 2011; 35: 1553-1560.
[10] Huh JB, Yang JJ, Choi KH, Bae JH, Lee JY, Kim SE, Shin SW. Effect of rhBMP-2 immobilized anorganic bovine bone matrix on bone regeneration. Int J Mol Sci 2015; 16: 16034-16052.
[11] Urist MR. Bone: formation by autoinduction. Science 1965; 150: 893-899.
[12] Mauney JR, Jaquiéry C, Volloch V, Heberer M, Martin I, Kaplan DL. In vitro and in vivo evaluation of differentially demineralized cancellous bone scaffolds combined with human bone marrow stromal cells for tissue engineering. Biomaterials 2005; 26: 3173-3185.
[13] Zomorodian E, Baghaban Eslaminejad M. Mesenchymal stem cells as a potent cell source for bone regeneration. Stem Cells Int 2012; 2012: 1-9.
[14] Saeed H, Ahsan M, Saleem Z, Iqtedar M, Islam M, Danish Z, Khan AM. Mesenchymal stem cells (MSCs) as skeletal therapeutics - an update. J Biomed Sci 2016; 23: 1-15.
[15] Yamaguchi Y, Ohno J, Sato A, Kido H, Fukushima T. Mesenchymal stem cell spheroids exhibit enhanced in-vitro and in-vivo osteoregenerative potential. BMC Biotechnol 2014; 14: 1-10.
[16] Mangano FG, Colombo M, Veronesi G, Caprioglio A, Mangano C. Mesenchymal stem cells in maxillary sinus augmentation: a systematic review with meta-analysis. World J Stem Cells 2015; 7: 976-991.
[17] Bornes TD, Adesida AB, Jomha NM. Mesenchymal stem cells in the treatment of traumatic articular cartilage defects: a comprehensive review. Arthritis Res Ther 2014; 16: 432.
[18] Wei X, Yang X, Han ZP, Qu FF, Shao L, Shi YF. Mesenchymal stem cells: a new trend for cell therapy. Acta Pharmacol Sin 2013; 34: 747-754.
[19] Li F, Wang X, Niyibizi C. Bone marrow stromal cells contribute to bone formation following infusion into femoral cavities of a mouse model of osteogenesis imperfecta. Bone 2010; 47: 546-555.
[20] Chatterjea A, Meijer G, van Blitterswijk C, de Boer J. Clinical application of human mesenchymal stromal cells for bone tissue engineering. Stem Cells Int 2010; 2010: 215625.
[21] Qi Y, Niu L, Zhao T, Shi Z, Di T, Feng G, Li J, Huang Z. Combining mesenchymal stem cell sheets with platelet-rich plasma gel/calcium phosphate particles: a novel strategy to promote bone regeneration. Stem Cell Res Ther 2015; 6: 256.
[22] Kang BJ, Ryu HH, Park SS, Koyama Y, Kikuchi M, Woo HM, Kim WH, Kweon OK. Comparing the osteogenic potential of canine mesenchymal stem cells derived from adipose tissues, bone marrow, umbilical cord blood, and Wharton's jelly for treating bone defects. J Vet Sci 2012; 13: 299-310.
[23] Chen W, Zhou H, Weir MD, Tang M, Bao C, Xu HH. Human embryonic stem cell-derived mesenchymal stem cell seeding on calcium phosphate cement-chitosan-RGD scaffold for bone repair. Tissue Eng Part A 2013; 19: 915-927.
[24] Haynesworth SE, Goshima J, Goldberg VM, Caplan AI. Characterization of cells with osteogenic potential from human marrow. Bone 1992; 13: 81-88.
[25] Li J, Guo W, Xiong M, Han H, Chen J, Mao D, Tang B, Yu H, Zeng Y. Effect of SDF-1/CXCR4 axis on the migration of transplanted bone mesenchymal stem cells mobilized by erythropoietin toward lesion sites following spinal cord injury. Int J Mol Med 2015; 36: 1205-1214.
[26] Xie H, Yang F, Deng L, Luo J, Qin T, Li X, Zhou GQ, Yang Z. The performance of a bone-de-

rived scaffold material in the repair of critical bone defects in a rhesus monkey model. Biomaterials 2007; 28: 3314-3324.
[27] Lei P, Sun R, Wang L, Zhou J, Wan L, Zhou T, Hu Y. A new method for xenogeneic bone graft deproteinization: comparative study of radius defects in a rabbit model. PLoS One 2015; 10: e146005.
[28] Hou GZ, Xu F, Li WJ, Zhu XM, Song XH, Zhan YL. Expression of bone morphogenetic protein 2 in rabbit radial defect site with different lengths. Int J Clin Exp Med 2015; 8: 9229-9238.
[29] Wang F, Su XX, Guo YC, Li A, Zhang YC, Zhou H, Qiao H, Guan LM, Zou M, Si XQ. Bone regeneration by nanohydroxyapatite/chitosan/poly (lactide-co-glycolide) scaffolds seeded with human umbilical cord mesenchymal stem cells in the calvarial defects of the nude mice. Biomed Res Int 2015; 2015: 261938.
[30] Glatt V, Bartnikowski N, Quirk N, Schuetz M, Evans C. Reverse dynamization: influence of fixator stiffness on the mode and efficiency of large-bone-defect healing at different doses of rhBMP-2. J Bone Joint Surg Am 2016; 98: 677-687.
[31] Fong EL, Chan CK, Goodman SB. Stem cell homing in musculoskeletal injury. Biomaterials 2011; 32: 395-409.
[32] Fernandes MB, Guimaraes JA, Casado PL, Cavalcanti AS, Goncalves NN, Ambrosio CE, Rodrigues F, Pinto AC, Miglino MA, Duarte ME. The effect of bone allografts combined with bone marrow stromal cells on the healing of segmental bone defects in a sheep model. BMC Vet Res 2014; 10: 36.
[33] Liu X, Liao X, Luo E, Chen W, Bao C, Xu HH. Mesenchymal stem cells systemically injected into femoral marrow of dogs home to mandibular defects to enhance new bone formation. Tissue Eng Part A 2014; 20: 883-892.
[34] Knight MN, Hankenson KD. Mesenchymal stem cells in bone regeneration. Adv Wound Care (New Rochelle) 2013; 2: 306-316.
[35] Im JY, Min WK, You C, Kim HO, Jin HK, Bae JS. Bone regeneration of mouse critical-sized calvarial defects with human mesenchymal stem cells in scaffold. Lab Anim Res 2013; 29: 196-203.
[36] Alam S, Ueki K, Marukawa K, Ohara T, Hase T, Takazakura D, Nakagawa K. Expression of bone morphogenetic protein 2 and fibroblast growth factor 2 during bone regeneration using different implant materials as an onlay bone graft in rabbit mandibles. Oral Surg Oral Med Oral Pathol Oral Radiol Endod 2007; 103: 16-26.
[37] Han Q, Ding J, Zheng Y, Zhuang X, Chen X, Wang J. Hydroxyapatite and vancomycin composited electrospun polylactide mat for osteomyelitis and bone defect treatment. J Control Release 2015; 213: e92.
[38] Heymann D, Delecrin J, Deschamps C, Gouin F, Padrines M, Passuti N. [In vitro assessment of combining osteogenic cells with macroporous calcium-phosphate ceramics]. Rev Chir Orthop Reparatrice Appar Mot 2001; 87: 8-17.
[39] Boos AM, Loew JS, Deschler G, Arkudas A, Bleiziffer O, Gulle H, Dragu A, Kneser U, Horch RE, Beier JP. Directly auto-transplanted mesenchymal stem cells induce bone formation in a ceramic bone substitute in an ectopic sheep model. J Cell Mol Med 2011; 15: 1364-1378.
[40] Lohberger B, Payer M, Rinner B, Bartmann C, Stadelmeyer E, Traunwieser E, DeVaney T, Jakse N, Leithner A, Windhager R. Human intraoral harvested mesenchymal stem cells: characterization, multilineage differentiation analysis, and 3-dimensional migration of natural bone mineral and tricalcium phosphate scaffolds. J Oral Maxillofac Surg 2012; 70: 2309-2315.
[41] Wu G, Hunziker EB, Zheng Y, Wismeijer D, Liu Y. Functionalization of deproteinized bovine bone with a coating-incorporated depot of BMP-2 renders the material efficiently osteoinductive and suppresses foreign-body reactivity. Bone 2011; 49: 1323-1330.
[42] Baldini N, De Sanctis M, Ferrari M. Deproteinized bovine bone in periodontal and implant surgery. Dent Mater 2011; 27: 61-70.
[43] Makridis KG, Ahmad MA, Kanakaris NK, Fragkakis EM, Giannoudis PV. Reconstruction of iliac crest with bovine cancellous allograft after bone graft harvest for symphysis pubis arthrodesis. Int Orthop 2012; 36: 1701-1707.
[44] Park JY, Koo KT, Kim TI, Seol YJ, Lee YM, Ku Y, Rhyu IC, Chung CP. Socket preservation using deproteinized horse-derived bone mineral. J Periodontal Implant Sci 2010; 40: 227-231.
[45] Anselme K. Osteoblast adhesion on biomaterials. Biomaterials 2000; 21: 667-681.